Structural Engineering and Mechanics, *Vol. 65, No. 3 (2018) 315-325*
DOI: https://doi.org/10.12989/sem.2018.65.3.315

Prediction of flexural behaviour of RC beams strengthened with ultra high performance fiber reinforced concrete

Ramachandra Murthy A[1], M. Aravindan[2] and P. Ganesh*[2]

[1]*CSIR-Structural Engineering Research Centre, Chennai, India, 600113*
[2]*AcSIR, CSIR-Structural Engineering Research Centre, Chennai, India, 600113*

(Received July 20, 2017, Revised November 14, 2017, Accepted November 28, 2017)

Abstract. This paper predicts the flexural behaviour of reinforced concrete (RC) beams strengthened with a precast strip of ultra-high performance fiber-reinforced concrete (UHPFRC). In the first phase, ultimate load capacity of preloaded and strengthened RC beams by UHPFRC was predicted by using various analytical models available in the literature. RC beams were preloaded under static loading approximately to 70%, 80% and 90% of ultimate load of control beams. The models such as modified Kaar and sectional analysis predicted the ultimate load in close agreement to the corresponding experimental observations. In the second phase, the famous fatigue life models such as Papakonstantinou model and Ferrier model were employed to predict the number of cycles to failure and the corresponding deflection. The models were used to predict the life of the (i) strengthened RC beams after subjecting them to different pre-loadings (70%, 80% and 90% of ultimate load) under static loading and (ii) strengthened RC beams after subjecting them to different preloading cycles under fatigue loading. In both the cases precast UHPFRC strip of 10 mm thickness is attached on the tension face. It is found that both the models predicted the number of cycles to failure and the corresponding deflection very close to the experimental values. It can be concluded that the models are found to be robust and reliable for cement based strengthening systems also. Further, the Wang model which is based on Palmgren-Miner's rule is employed to predict the no. of cycles to failure and it is found that the predicted values are in very good agreement with the corresponding experimental observations.

Keywords: RC beam; static loading; pre-damage; ultra high performance fiber reinforced concrete; retrofitting; fatigue loading; analytical models

1. Introduction

Deterioration of Reinforced Concrete (RC) structures manifests through the strength and stiffness degradation of their members which is mainly attributed to the material heterogeneity, aging, corrosion of steel reinforcement, accidental impacts and the environment. This necessitates a dire requirement for the strengthening of existing RC structures either by enhancing the load carrying capacity or by improving the in-service performance. Repair and retrofitting have garnered prominence over the last two decades for this reason. Some structures/ components such as bridge girders, slabs in parking garages, airport pavements and machine foundations are generally subjected to fatigue loading in the form of repeated loads during their service lifetime. This type of loading may cause failure even when the nominal peak loads are smaller than the ultimate capacity of the structure (Manfredi and Pecce 1997, Deng 2005, Wang *et al.* 2006, Cheng *et al.* 2011).

The popular techniques for repair and retrofitting of damaged RC structures using jacketing, post-tensioning, bonded steel plates and carbon fibre reinforced plastics (CFRP) were investigated by various researchers (Shahawy and Beitelman 1999, Dong *et al.* 2012, El-Refai *et al.* 2012, Shannag *et al.* 2014). The various limitations of the above methods include, (i) undesirable shear failures, (ii) difficulty in handling heavy steel plates, (iii) corrosion of steel, (iv) the need for butt joint systems because of limited workable lengths and (v) brittle failure due to mismatch of tensile strength and stiffness with that of concrete and retrofitting materials (Nanni 1995, Buyukozturk and Hearing 1998, Bakis *et al.* 2002, Dong *et al.* 2011, Attari 2012).

In view of the specific limitations of the above methods, a new fibre reinforced ultra-high performance concrete with high mechanical and durability properties was proposed as a suitable choice for retrofitting (Alaee and Karihaloo 2003a, 2003b, Xu *et al.* 2012, Shin *et al.* 2015, Kevin *et al.* 2015, Prem *et al.* 2015). This material possesses a unique combination of low permeability, improved homogeneity, ductility, high strength, high tensile strength and high toughness. Ultra high performance fibre reinforced concrete (UHPFRC) has also found to be excellent bond with normal concrete (Almusallam and Salloum 2001, Alaee and Karihaloo 2003a, Benson and Karihaloo 2005, Leung *et al.* 2007, Xu *et al.* 2012, Ramachandra Murthy *et al.* 2013, Kevin *et al.* 2015, Shin *et al.* 2015, Prem *et al.* 2016).

Although it is a fact that UHPFRC has been recognized as a potential candidate for repair and retrofitting of RC

*Corresponding author, Research Scholar
E-mail: ganesh@acsir.res.in
[a]Scientist
[b]Former PG Student

ISSN: 1225-4568 (Print), 1598-6217 (Online)

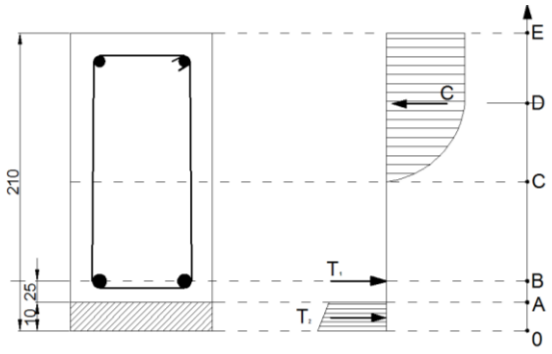

Fig. 1 Stress diagram of the strengthened RC beam

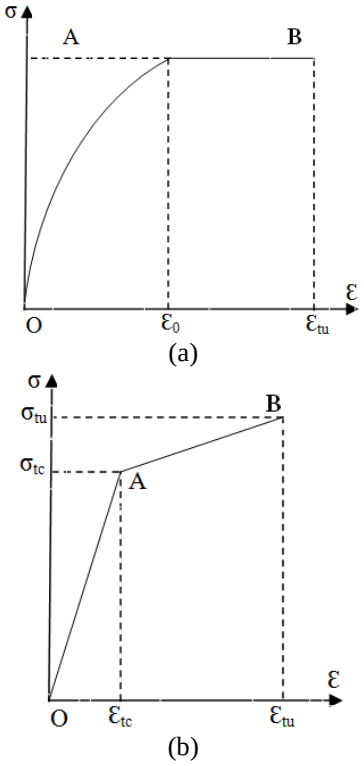

Fig. 2 Idealized stress strain diagrams for material used in beams (a) compressive stress- strain curve of normal strength concrete (b) Tensile stress-strain curve of UHPFRC

structures about a decade ago, only few analytical studies were reported for response prediction of strengthened RC members with UHPFRC strip under static and fatigue loading. The present study provides the useful information on various analytical models to predict the response behaviour of strengthened RC beams with UHPFRC strip.

2. Various analytical models

This section discusses the various analytical models employed in the present study for response prediction of strengthened RC beams strengthened with UHPFRC

2.1 Moment carrying capacity of the section

Sectional analysis approach can be used to find out the ultimate moment carrying capacity of retrofitted RC flexural members. Fig. 1 shows the typical section of RC beam strengthened with UHPFRC on tension face. Various forces and the nature of forces are indicated in Fig. 1.

The main assumptions made in this method are as follows:

• Plane cross section remains plane after bending, i.e. plane section assumption.

• Perfect integral behaviour between the pre-damage concrete and UHPFRC overlay, i.e., no debonding of overlay.

Fig. 2 presents the constitutive relationship of normal strength concrete under compression and constitutive relationship of UHPFRC under tension.

where,

$\mathcal{E}_0$ = Strain corresponding to f_{ck}

f_{ck} = Characteristic compressive strength of cubes

$\mathcal{E}_{cu}$ = Ultimate compressive strain

σ_{tu} = Tensile strength of concrete

σ_{tc} = Tensile stress corresponding to 90% of σ_{tu}

$\mathcal{E}_{tc}$ = Strain corresponding to σ_{tc}

$\mathcal{E}_{tu}$ = Strain corresponding to σ_{tu}

• The tensile contribution of the concrete is simplified as bilinear model, where in ultimate tensile strength is to be obtained from experiments. The stress-strain model of the concrete under uniaxial compression

$$\sigma_c = f_c\left[2\frac{\varepsilon_{cu}}{\varepsilon_o} - \left(\frac{\varepsilon_{cu}}{\varepsilon_o}\right)^2\right]; \text{(compressive) for } 0 \le \varepsilon_c \le \varepsilon_{o]}$$

$\sigma_c = f_c$; (compressive) for $\varepsilon_o \le \varepsilon_{cu} \le \varepsilon_u$

• The tensile stress-strain curve for UHPFRC under uniaxial tension

$$\sigma_t = \left[\frac{\sigma_{tc}}{\varepsilon_{tc}}\varepsilon_t\right]; \text{ for } 0 \le \varepsilon_t \le \varepsilon_{tc}$$

$$\sigma_t = \left[\sigma_{tc} + \frac{\sigma_{tu} - \sigma_{tc}}{(\varepsilon_{tu} - \varepsilon_{tc})}(\varepsilon_{tu} - \varepsilon_{tc})\right]; \text{ for } \varepsilon_{tc} \le \varepsilon_t \le \varepsilon_{tu}$$

• In accordance with the elastic bending theory, the tensile contribution of the concrete is completely neglected; the experimental observation showed that the initiated cracks (flexural and shear) are not propagated beyond the limiting depth of the neutral axis due to the pre-load applied on the RC beams. Hence it is assumed that for the analysis of strengthened pre-loaded beams, elastic beam theory is applicable to estimate moment carrying capacity.

2.1 Alaee and Karihaloo model (2003)

Alaee and Karihaloo (2003) proposed an analytical model to predict the ultimate flexural capacity of the section by considering the dominant flexural crack in the beam through fracture mechanics approach. To model the dominant flexural crack, bridging force across the crack faces from the reinforcing steel, post-peak tension softening response of concrete, bridging stresses in the retrofit strips in addition to the oments were comnsidered (Fig. 3).

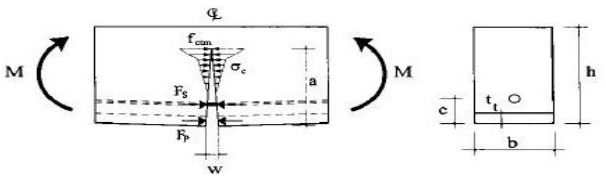

Fig. 3 Free body diagram of dominant flexural crack in retrofitted beams (Alaee and Karihaloo 2003)

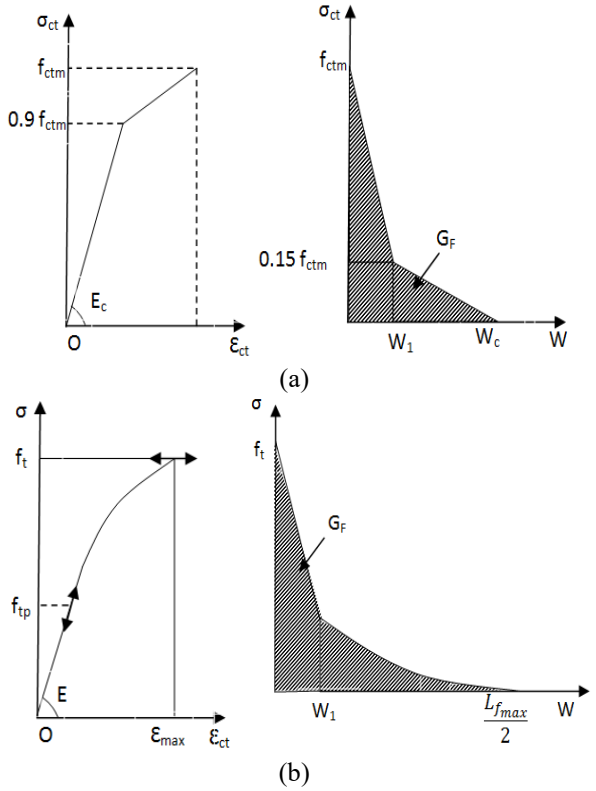

Fig. 4 Stress-deformation diagrams proposed by CEB-FIP Model Code (1993) for (a) concrete (b) CARDIFRC (Alaee *et al.* 2003)

To simplify the computations, it is assumed that the crack profile is always linear and it is specified by its depth (a) and the opening (w) at its mouth. It is assumed that concrete even after the attainment of its tensile strength, is capable of carrying residual tensile stresses due to its tension softening behaviour. The amount of the stress transmitted along the crack faces depends upon the crack opening; it decreases with an increase in the crack opening. As shown in Fig. 3, the residual tensile stress in concrete (σ_c), acts as a closure pressure on the dominant crack faces. This stress varies from f_{ctm},the tensile strength of concrete at the crack tip, to nothing where the crack opening equals the critical crack opening of concrete as shown in Fig. 4. Similar to concrete, even the retrofit strips produce closure pressure at the face of cracks due to tension softening.

To calculate the moment resistance of the retrofitted beams M_F, the condition of the dominant crack at the maximum load is taken as the crucial parameter. The bridging force from steel F_S is the most significant closing force on the crack faces. There is no definite relationship between the geometrical properties of the crack (w and a) and the bridging force in steel. However, there are some empirical relations which exist for the same in the literature. Details are given below.

2.1.1 Carpinteri's approximation

Bosco and Carpinteri (1992) assumed that the displacement discontinuity in a cracked cross section at the level of reinforcement is zero up to the moment of yielding or slippage of the reinforcement. They considered a rigid perfectly plastic behaviour of the reinforcement and the moment is obtained at plastic flow or slippage. In fact, they assumed that the reinforcement steel yields as soon as the crack at this level starts to open. According to this assumption, the bridging force exerted by steel is given by,

$$F_s = A_s f_y \tag{1}$$

where f_y =yield stress of the reinforcing bar; and A_s =area of steel. The steel force is therefore uncoupled from the crack opening displacement at the level of steel.

2.2.2 Kaar's formula

Kaar and Mattock (1963) expressed the tensile stress in steel as a function of the crack width w_s at the level of deformed bar reinforcement which is given by,

$$f_s = \frac{F_s}{A_s} = \frac{11876.5 w_s}{A^{1/4}} \tag{2}$$

where A=area of concrete surrounding each bar ($A=A_e/n$, where n is the number of bars) and f_s, $w_s$and A are in MPa, mm and mm^2, respectively.

2.2.3 Modified Kaar formula

Lange-Kornbak and Karihaloo (1999) conducted an experimental program and compared the test results with approximate nonlinear fracture mechanical prediction of the ultimate capacity of three-point bend, singly reinforced concrete beams. They found that Kaar's formula overestimates the crack opening by the factor of 3.5-4. Due to the relative similarity between the properties of the beam and those obtained from the experimental program, Kaar's formula was improved by calibrating the results against the test data with the least variation. The calibration suggested the following relationship between the tensile stress in steel and the crack width at the level of deformed bar

$$f_s = \frac{F_s}{A_s} = \frac{4.8 \text{ x } 11876.5 w_s}{A^{1/4}} \tag{3}$$

It can be observed that the right-hand side of Eq. (3) has increased by a factor of 4.8 in comparison with the original Kaar's formula. As a result, the bridging force exerted by steel reinforcement in this case is higher than that based on Kaar's formula in Eq. (2) and it can therefore be expected that this modification increases the moment resistance of the beams in comparison with that of Kaar's formula. To obtain the moment carrying capacity of the section, the moment (M) has to be related to the crack depth (a) and crack mouth opening (w) through the conditions of smooth closure of cracks and crack opening compatibility equation.

It is assumed that stress at the crack tip is finite as per

Barenblatt cohesive crack model (1959) considering the cohesive zone (c) near the crack tip is very much smaller than the crack depth (a).This leads to the condition that the net Stress Intensity Factor(K_I) at the crack tip which is obtained by superposing SIF produced at the crack tip due to moment(K_{IM}), closure forces exerted by steel(K_{IS}), concrete(K_{Iconc}) and retrofit strip (K_{Istrip}) is zero.

$$K_{IM} - K_{IS} - K_{Iconc} - K_{Istrip} = 0 \quad (4)$$

K_{IM} can be calculated from the formula given by Guinea *et al.* (1998) and the other stress intensity factors can be evaluated directly or with integration from the relation proposed by Tada *et al.* (1985). In addition to the condition of smooth closure of crack faces at its tip, the compatibility of crack opening displacement of a retrofitted beam at the level of steel reinforcement has also to be considered (Leung 1998)

$$(w_s)_M - (w_s)_s - (w_s)_{conc} - (w_s)_{strip} = w_s \quad (5)$$

where $(w_s)_i$are the crack mouth opening displacements at the level of steel bar produced by the moment, closure forces exerted by steel, concrete and retrofit strip. Complete details can be found in Alaee *et al.* (2003).

2.3 Deflection of beams subjected to fatigue loading

When concrete beams subjected to a fatigue loading, the deflection generally increases significantly with increase of loading cycles. It is essential to predict the behaviour of the specimens under fatigue loading in order to fix the safety and serviceability limits. In addition, excessive deflection will cause the impending failure. In certain cases there could be change in stress in reinforcement due to creeping of concrete.

2.3.1 Papakonstantinou model (2002)

Papakonstantinou *et al.* (2002) proposed an analytical model to predict the deflection of reinforced concrete beams strengthened with high strength fibre reinforced composite fabric. The model can also be used to compute any changes in stresses due to cyclic creep of concrete. Balaguru and Shah (1982) presented an analytical model to predict the deflection of reinforced concrete beams subjected to fatigue loading. Based on this model, the two major contributing factors are cyclic creep of concrete and degradation of flexural stiffness due to increase in cracking and reduction in modulus of rupture under fatigue loading.

The cyclic creep strain of concrete can be expressed as the sum of two strain components; a mean strain component, based on $\sigma_m = ((\sigma_{max} + \sigma_{min})/2)\ /f_c'$, and a cyclic strain component, based on $\Delta=(\sigma_{max} - \sigma_{min})/f_c'$.

Based on the above terms, a regression equation based on several experimental results from the literature was obtained as

$$\varepsilon_c = 129.\sigma_m.t^{1/3}+17.8.\sigma_m.\ \Delta.\ N^{1/3} \quad (6)$$

where ε_c is the cyclic creep strain in micro mm/mm

Δ is the stress range expressed as a fraction of the compressive strength

σ_m is the mean stress expressed as a fraction of the compressive strength

σ_{max} is the maximum applied compressive stress in concrete

σ_{min} is the minimum applied compressive stress in concrete

N is the number of cycles

t is the time from start of loading in hours.

Using the value of cyclic strain, the cycle dependent secant modulus for concrete in compression, E_N can be calculated from the equation given below

$$E_N = \frac{\sigma_{max}}{\frac{\sigma_{max}}{E} + \varepsilon_c} \quad (7)$$

where E is the initial secant modulus

E_N is the cyclic modulus after N number of cycles

The modulus of rupture of concrete is calculated using the equation as follows

$$f_{r,N} = f_r\left(1 - \frac{log_{10}N}{10.954}\right) \quad (8)$$

From the above equation, cracking moment $M_{cr,N}$ can be computed from bending equation and which in turn can be used to find the effective moment of inertia of the cracked section after N number of cycles,$I_{e,N}$.

Now given the static moment M_a, cyclic modulus E_N and effective moment of inertia $I_{e,N}$ the deflection δ for the given loading configuration of the test can be computed. The limitation of this model is that it cannot be used to predict the deflections at the point of failure since the deflection shoots to maximum either by yielding of reinforcement or the crushing of concrete.

2.3.2 Ferrier model (2011)

Along the similar lines of model of Papakonstantinou (2002), Ferrier (2011) proposed an analytical procedure to study the serviceability aspect of the reinforced concrete beams strengthened with composite material. Although this model uses the same expression for calculating the cycle dependent secant modulus of the concrete in compression given in equation (7), the values of the tensile strain of steel are determined separately in addition to the compressive strain of the concrete considering the effect of number of cycles. The analytical procedure to determine the cycle-dependent deflection of the reinforced concrete beams is the same as the above discussed model except for the expressions considered for the determination of cycle-dependent strains of concrete and steel.

The value of concrete compressive strain (ε_{cn}) expressed as a function of number of load cycles which can be used to find the cycle-dependent modulus of elasticity of concrete is given as follows

$$\varepsilon_{cn} = 8.417 \times 10^6 \times \left(\frac{\sigma_c^m}{f_c}\right) \times \left[\left(\frac{N}{\omega}\right)^{1/3} + 3.87 \times \left(\frac{\sigma_c^r}{f_c}\right)\left(\frac{N}{9.75}\right)^{1/3}\right] \quad (9)$$

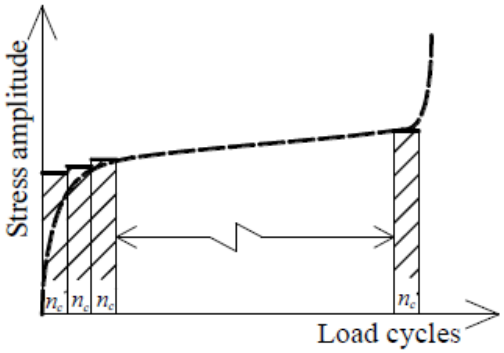

Fig. 5 Discretization of steel stress amplitude

where

ω is the frequency of the loading in Hz

N is the number of cycles

f_c is the strength of the concrete in MPa

$\sigma_c^m = (\sigma_{max} - \sigma_{min})/2$ is the average loading stress

$\sigma_c^r = \sigma_{max} - \sigma_{\min}$ is the stress cycle amplitude

Similarly, the steel strain ε_{sn} expressed as a function of number of cycles at failure (N_f), steel yield strength (f_y) and ultimate strain (ε_{su}) is given as follows

$$\varepsilon_{sn} = \frac{f_y}{E} \times (2N_f)^b + \varepsilon_{su} \times (2N_f)^c \tag{10}$$

Where b and c are material constants taken from Ferrier *et al.* (2011).

Once the values of strains are known, the neutral axis can be determined using sectional analysis approach of concrete sections after which the deflections can be found from the static moment M_a,cyclic modulus E_N and the effective moment of inertia $I_{e,N}$ described in the previous model.

2.3.3 Wang model (2015)

When the tensile face of RC beam is subjected to high strain levels, the beam cracks and the stresses are redistributed. Therefore, the real stresses acting on each material are not the same as those calculated by simplified models.

Wang *et al.* (2015) proposed an analytical model based on the failure criterion of steel reinforcement fracture, for predicting the fatigue life of reinforced concrete (RC) beam strengthened with fibre reinforced polymer (FRP) sheets. This model was constructed with the fiber section method and taken into the consideration of fatigue damage of the concrete.

In this model, the load cycle is divided into some loading blocks evenly and the stress amplitude of the tensile steel reinforcement is thought to be invariable in each loading block as shown in Fig. 5. Considering the degradation of material performance, including concrete creep, the stress amplitude of the tensile steel reinforcement is obtained by using the traditional sectional analysis method. Therefore, the fatigue life of the strengthened beam is predicted by using the well-known Palmgren-Miner rule. The model takes into account the degradation of the component material performance as well as the creep of concrete. The debonding of the strip is ignored in this model assuming perfect bond between the concrete substrate and the strip.

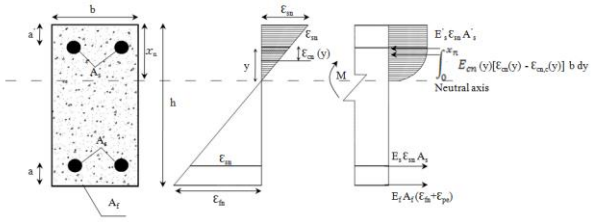

Fig. 6 Strain-stress distribution

Before the stress amplitude of each loading block is determined using the sectional analysis method, the following assumptions are made: 1) Plane sections are considered to remain plane during the fatigue loading. This assumption is reasonable because an approximately linear strain distribution along the beam height was experimentally observed during the fatigue loading (Shahawy *et al.* 1999); 2) No bond-slip is assumed between concrete and other component materials (i.e., steel reinforcement and the strip); and 3) Due to the low tensile strength of concrete, the tension role of concrete is ignored in the calculation.

A cracked section of the concrete is shown in Fig. 6.

Then, based on the sectional equilibrium of external and internal forces and moments, the following equations can be expressed as follows

$$\begin{aligned} P = {} & E_s\varepsilon_{sn}A_s + E_f(\varepsilon_{fn} \\ & + \varepsilon_{pi})A_{f-}\int_0^{x_n} E_{cn}(y)[\varepsilon_{cn}(y) \\ & - \varepsilon_{cn,c}(y)]bdy \end{aligned} \tag{11}$$

$$\begin{aligned} M = {} & E_s\varepsilon_{sn}A_s(h - x_n - a) \\ & + E_f(\varepsilon_{fn} + \varepsilon_{pi})A_f(h - x_n) \\ & + \int_0^{x_n} E_{cn}(y)[\varepsilon_{cn}(y) \\ & - \varepsilon_{cn,c}(y)]bydy \end{aligned} \tag{12}$$

where

- P is the axial force (here $P = 0$)
- $M$is the bending moment
- x_n is the depth of the compression zone for the concrete at n^{th} cycle
- $E_s$and E_f are the elastic modulii of the steel and the strip respectively
- $E_{cn}(y)$ is the effective elastic modulus of the specified concrete layer at n^{th} cycle
- $\varepsilon_{sn}$and ε_{fn} are the cycle-dependent strains due to fatigue loading
- $\varepsilon_{cn}(y)$and$\varepsilon_{cn,c}(y)$ are the total strain and the creep strain of the specified concrete layer at n^{th} cycle
- A_s and A_f are the cross-sectional areas of the steel reinforcement and the strip respectively

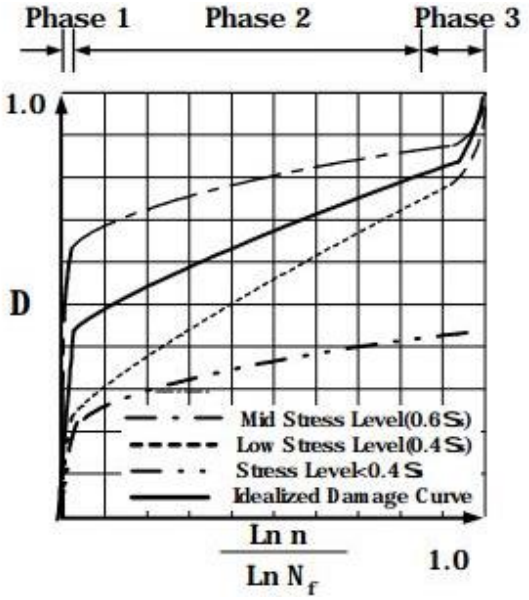

Fig. 7 Idealized damage accumulation

- b is the beam width
- a is the effective cover of the beam
- y is the distance between the centroid of the specified concrete layer and the neutral axis.

The fatigue life of strengthened RC beams can be predicted by the summation of the corresponding fatigue load cycles of each stress (according to Palmgren-Miner rule) until the rupture failure of tensile steel reinforcement occurs (i.e., D=1)

$$N_p = \sum n_i \tag{13}$$

where N_p is the predicted fatigue life of the specimen. Complete details can be found in Wang (2015)

2.4 Fatigue-damage inclusion in pre-damaged beam

It is absolutely necessary that the level of pre-damage in the beam is taken into account for predicting the behaviour of retrofitted beams. The effect of pre-damage can be introduced into a suitable analytical model by employing appropriate damage variables for a given problem. One such model based on the modification of cumulative damage theory was proposed by Hongseob *et al.* (2005).

2.4.1 Hongseob model (2005)

Classical damage mechanics principles do not bode well in the situations where boundary conditions keep changing as damage increases. Therefore, the method proposed herein is based on the empirical information provided by the load-deformation relationships studied from various literature involving the strengthening of beams with composite materials.

In a simple case, the fatigue damage shall be defined as follows

$$D = \frac{\delta}{\delta_{max}} \tag{14}$$

Table 1 Materials, mix proportion and mechanical properties

Concrete	Ingredients	Mix proportion	Curing	Mechanical properties
Normal strength concrete (NSC)	Ordinary Portland Cement 53 grade, natural sand, crushed aggregate size below 12 mm and potable water	Cement: Fine Aggregate: Coarse Aggregate: W/C 1:1.67:1.86:0.45	water at ambient temperature for 28 days	Comp. Strength = 35 MPa Split = 3.2 MPa Fracture energy = 185 N/m
Ultra High Performance Fibre Reinforced Concrete (UHPFRC)	Cement, Silica Fume, Quartz sand, Quartz Powder and Water Brass-coated steel fibers diameter 0.18 mm and length 13 mm	Cement: Silica Fume: Quartz Sand: Quartz powder: W/C 1:0.25:1.1:0.4:0.23 Steel fibers 2% by volume of concrete &the dosage of superplasticizer is 3.5%	Water curing at ambient temperature for 2 days, 200°C for 1 day. Later water curing till testing.	Comp. Strength= 122.5 MPa Split = 20.7 MPa Fracture energy = 13760 N/m

where δ is the displacement at any load cycle
δ_{max} is the maximum displacement prior to failure.

It is known that δ_{max} for cyclic loading is very similar to the maximum displacement observed in a static test, for both unstrengthened and strengthened beams (Hongseob *et al.* 2005).

But unlike the equation, the damage will not increase proportionately and it evolves in three phases which are given in Fig. 7.

The three damage phases mentioned in above figure are illustrated: In Phase I, consisting of about 10 cycles, the first load cycle introduces a considerable amount of damage, whereas the subsequent cycles of Phase II cause damage increments of decreasing magnitude. In Phase III, fatigue damage accelerates, leading to failure.

The damage of Phase I is mostly due to that caused in the first load cycle, which is similar to that produced in a static test with the same load, i.e.,

$$D_I = \frac{\delta_{static}}{\delta_{max}} n_I = 1 \; to \; 10 \tag{15}$$

where, δ_{max} is the maximum deflection value obtained from the experimental testing of control beam under fatigue loading.

Similarly, in Phase-II, the small increments in damage can be represented by

$$D_{II} = \beta \frac{\ln n_{II}}{\ln N_f} n_I < n_{II} \leq n_e \tag{16}$$

where N_f is the number of cycles to failure at a given stress level,

n_{II} is the number of load cycles applied

β is the slope of the damage curve

n_e is the number of cycles defining the end of Phase II.

n_e depends on the applied stress level and is assumed to be reached when the beam deflection under cyclic loading is equal to 90% of the maximum deflection observed in a static test.

$$\beta = -1.644 \ln\left(\frac{P}{P_s}\right) - 0.2955 \tag{17}$$

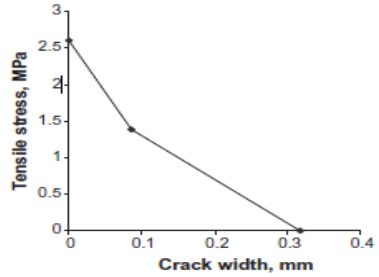

(a) NSC

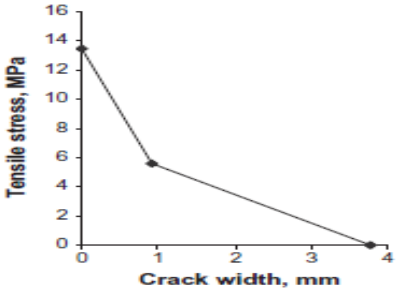

(b) UHPFRC

Fig. 8 Stress vs crack width relation for NSC and UHPFRC

The slope β in Phase II can be estimated from the test results for different stress levels and expressed in the form of a log function as follows:
where P is the upper limit of the applied fatigue load and P_s is the static failure load.

$$D_{III} = \gamma \frac{\ln(n_{III} - n_e)}{\ln N_f} n_e < n_{III} \leq N_f \tag{18}$$

where

$$\gamma = 0.445 \ln\left(\frac{P}{P_s}\right) + 0.6215 \tag{19}$$

Based on the level of fatigue pre-damage given to the beams, one of the three equations for damage can be used and the value of which is incorporated in the fatigue deflection models discussed in the previous section to assimilate the effect of damage in the analytical procedure.

3. Experimental studies

The experimental investigations were carried out on under-reinforced beams. Few beams were tested to failure to determine the failure load (control beams) and remaining beams were preloaded to different levels of damage by static loading. These beams were strengthened with precast UHPFRC strip on the tension face and tested to failure under constant amplitude loading. Another set of beams were subjected to fatigue predamage and then unloaded. After strengthening fatigue pre-damaged beams with UHPFRC strip, tested under constant amplitude fatigue loading.

Table 1 shows the details of materials, mixes and mechanical properties.

The yield strength of steel is 415 MPa. Stress vs crack width relation for NSC and UHPFRC is shown in Fig. 8.

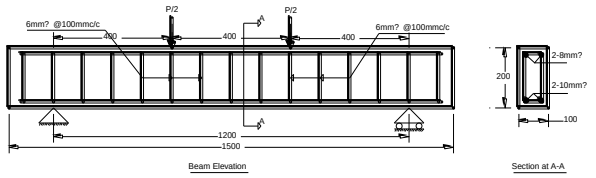

Fig. 9 Typical reinforcement details of RC beam

Table 2 Details of beams cast and tested

Type of Beam	Beam designation	Type of beam	Beam designation	Type of beam	Beam designation
Control beams (Static)	Average CBA	Preloaded to about 70% (static) & strengthened by Fatigue	SFB1 (2 beams)	Preloaded to about 90% (Static) & strengthened by fatigue	SFB3 (2 beams)
Control fatigue	FB1 FB2 Average FBA	Preloaded to about 80% (Static) & strengthened by fatigue	SFB2 (2 beams)	Fatigue pre-loaded to 10000 cycles & 20000 cycles, strengthened by fatigue	FFB1 (2 beams) FFB2 (2 beams)

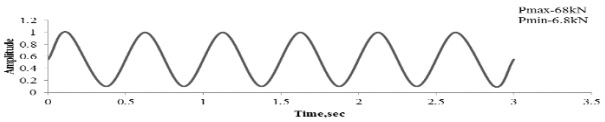

Fig. 10 Typical fatigue loading spectrum of control beam

3.1 Casting and testing of beams

The dimensions of the RC beam are 1500 mm (length) ×100 mm (width)×200 mm (depth). The reinforcement details of a typical RC beam including sectional view is shown in Fig. 9. Table 2 shows the details of all the beams cast and tested. The details include designation of the beam, degree of preloading and thickness of UHPFRC strip for retrofitting. In view of previous experience, it was decided to retrofit all the pre-damaged beams with 10 mm UHPFRC strip.

The average cracking load, yielding load and ultimate loads of control beam (CBA) are 33.21 kN, 71.34 kN and 77.84 kN, respectively. The average vertical deflection corresponding to yielding load and ultimate load are 6.67 mm and 14.13 mm, respectively. The average maximum deflection is 29.10 mm.

All the fatigue beams were tested under sinusoidal fatigue loading with a frequency of 2 Hz and stress ratio 0.1 (Figure 10). The maximum load is 68.0 kN and the minimum load is 6.8 kN. During testing, deflection and number of cycles to failure were recorded.

3.2 Strengthening scheme

UHPFRC strips (1500 mm×100 mm×10mm, length×width×thickness) were made using the mix proportions already mentioned above. All the pre-loaded beams were retrofitted with UHPFRC strips 10 mm thick, as per Table 1. Retrofitted beams were tested under displacement control in four-point bending. The retrofitted beams SFB1, SFB2, SFB3, FFB1 and FFB2 were tested under fatigue loading with stress ratio 0.1 (maximum load = 68 kN and the minimum load = 6.8 kN) and the responses such as central vertical deflection and fatigue cycles were

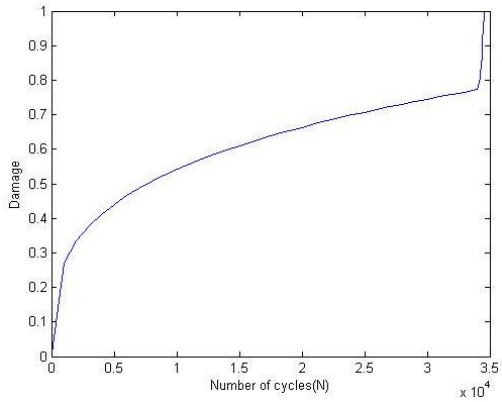

Fig. 11 Damage evolution with number of cycles

captured during the experiment. Fig. 11 shows the damage evolution with the number of cycles for the control specimen FBA. The same kind of damage propagation is observed in the specimens tested under fatigue loading. Damage here in this case refers to the ratio of the value of strain at a particular cycle of fatigue loading to ultimate value of the strain corresponding to the failure cycles (Liu *et al.* 2016).

Although concrete exhibits the similar behaviour under the fatigue loading, it seems sensible to choose strain of steel as a parameter of damage because the governing mode of failure is dictated by the steel reinforcement.

The damage D in this case can be defined by the following equation,

$$D = \frac{\varepsilon_{st,N}}{\varepsilon_{st,N_f}} \tag{20}$$

where, ε_{st}, N is the strain in the steel reinforcement corresponding to a specific number of cycles.

ε_{st}, N_f is the strain in the steel reinforcement corresponding to the failure number of cycles.

It can be seen from Fig. 11, that almost 60% of the damage occurs in the stable propagation zone of the curve (Zone-II) spanned over more than 30000 cycles whereas in the rapid propagation zone (Zone-III), the damage increases by 25% just over the span of less than 1000 cycles. The reason for Zone-II is the sustenance due to the steel reinforcement after it has yielded but once a certain number of cycles is reached, the limiting strain of the reinforcement is reached which leads to the failure of the reinforcement before the failure of the concrete. The strain values of the steel reinforcement are taken from the mean of two strain gauges attached to the reinforcement and for brevity only the damage curve of the control specimen is presented.

4. Results and discussion

4.1 Load carrying capacity

Ultimate load carrying capacity predicted by using various models such as Carpinteri, Kaar and Modified Kaar formulae and sectional analysis is compared with the experimental value (Table 3).

Table 3 Ultimate load capacity by using various models

Model/Approach	Ultimate load (kN)			
	Control beams	Strengthened beams (70% predamage)	Strengthened beams (80% predamage)	Strengthened beams (90% predamage)
Experimental	77.84	78.50	80.39	82.36
Carpinteri	78.35	85.26	88.72	89.92
Kaar	60.62	77.89	81.34	83.45
Modified Kaar	72.56	82.21	83.79	86.72
Sectional analysis	70.84	72.36	74.67	78.43

Table 4 Predicted fatigue life by analytical model

Beams		No of Cycles	Deflection, mm
FBA	Experimental	35594	15.44
	Papakonstantinou's model	34628	5.71
	Ferrier's model	34546	6.03
	Palmgren-Miner, Wang model (2015)	35213	--------
SFB1	Experimental	88229	13.64
	Papakonstantinou's model	92692	4.65
	Ferrier's model	94145	5.21
	Palmgren-Miner, Wang model (2015)	94254	
SFB2	Experimental	82152	13.64
	Papakonstantinou's model	80309	4.69
	Ferrier's model	80502	5.06
	Palmgren-Miner, Wang model (2015)	78456	
SFB3	Experimental	80698	13.61
	Papakonstantinou's model	82163	3.92
	Ferrier's model	82163	4.24
	Palmgren-Miner, Wang model (2015)	80656	
FFB1	Experimental	74026	13.42
	Papakonstantinou's model	74320	4.65
	Ferrier's model	74162	4.76
	Palmgren-Miner, Wang model (2015)	67123	
FFB2	Experimental	50800	11.21
	Papakonstantinou's model	51057	4.10
	Ferrier's model	50717	4.45
	Palmgren-Miner, Wang model (2015)	48897	

From Table 3, it can be observed that the ultimate load predicted by sectional analysis is in good agreement with the experimental observations and Carpinteri model overestimates the ultimate load. The reason could be due to the assumption that the steel yields as soon as the crack at the level of the steel reinforcement starts to open thus over-predicting the load capacity. Modified Kaar formula fairly predicts the ultimate load carrying capacity.

4.2 Fatigue deflection behavior

The models proposed by Papakonstantinou (2002) and Ferrier *et al.* (2010) were used to predict the deflection of RC beams strengthened with UHPFRC strip against number of cycles. These models account for the stiffness

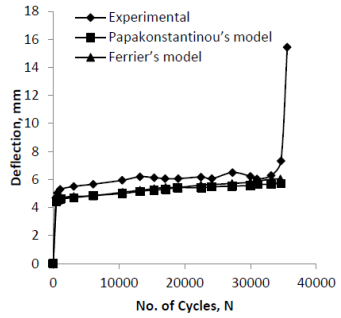

Fig. 12 No. of cycles vs deflection - FBA

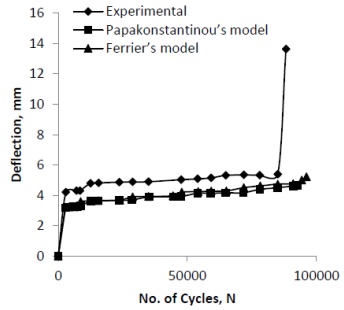

Fig. 13 No. of cycles vs deflection - SFB1

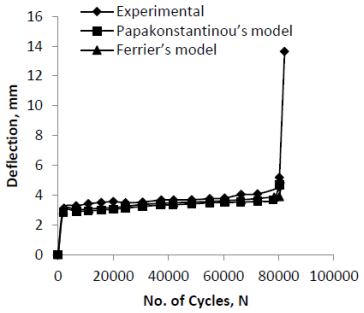

Fig. 14 No. of cycles vs deflection - SFB2

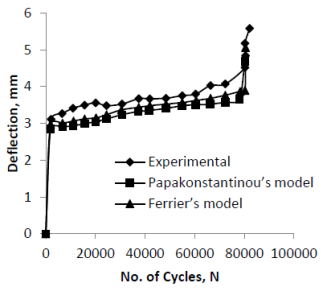

Fig. 14(a) No. of cycles vs deflection - SFB2 (Before phase 3)

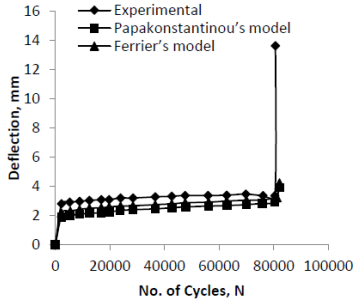

Fig. 15 No. of cycles vs deflection - SFB3

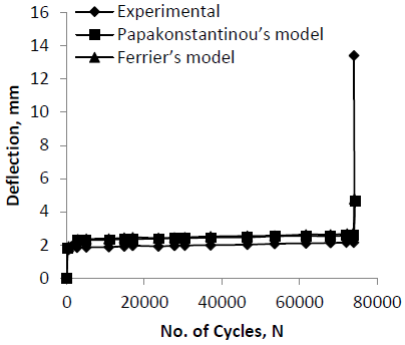

Fig. 16 No. of cycles vs deflection - FFB1

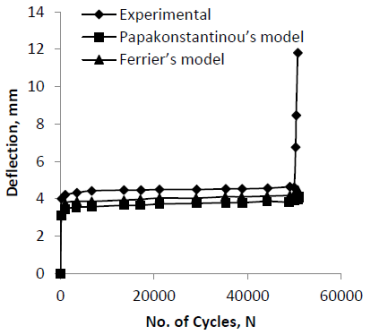

Fig. 17 No. of cycles vs deflection - FFB2

degradation for each cycle and determine the deflection at specific number of cycles using the cycle dependent secant modulus of the material. In addition, Ferrier *et al.* (2010) also considers the effect of number of cycles at failure and ultimate strain in the explicit expression for the cycle-dependent steel strain. Fatigue life has been predicted for all the retrofitted beams. Table 4 consolidates the responses such as number of cycles to failure and the deflection for all the tested beams and the predictions obtained from Papakonstantinou (2002) and Ferrier *et al.* (2010) models. From Table 4, the general observation is that the predictions obtained from the models are in reasonably very good agreement with the corresponding experimental values. The percentage difference between the experimental and the predicted values is in the range of 5 to 12%.

Figs. 12 to 17 show the variation of deflection with no. of cycles of experimental and predicted values by using the analytical models.

From Figs. 12 to 17, it can be clearly observed that deflections predicted by both the models are in very good agreement with the corresponding experimental observations. The predicted variation of no. of cycles vs deflection is in similar trend of experimental observations till the beginning of phase 3 (refer to Fig. 7).

For example, for the case of SFB3 (Fig. 14 and Fig. 14(a)), the experimental deflection just beginning of phase 3 is 3.4 mm. The corresponding cycles are 80455. The predicted deflection by Papakonstantinou's model corresponding to same number of cycles is 3.1 mm and by Ferrier's model is 3.2 mm. It can be confidently consolidated that the models are capable of predicting the deflection till the beginning of phase 3 of the failure of corresponding experimental beams. In some cases, the

predicted responses are marginally higher side or lower side w.r.t experimental values. This may be attributed to the nature of the damage expression chosen to represent the static damage imposed on the beams before strengthening. The very important observation is that although the models were originally developed to address the serviceability of CFRP and GFRP laminates, from the present investigation, it can be concluded that the models could also be used for prediction of the behaviour of cement based composite system as it is seen that the models could predict reliable results for the cement based composite strip systems. Further, the Wang model based on Palmgren-Miner's rule predicts the no. of cycles to failure as close to as experimental observations.

5. Summary

Various analytical models were reviewed for the prediction of the behaviour of retrofitted RC beams with UHPFRC. From the predictions, it can be summarized that

(i) By sectional analysis and modified Kaar formula, the predicted ultimate load is comparable with the corresponding experimental observations

(ii) The predicted no. of cycles vs deflection trend by both the models, namely, Papakonstantinou and Ferrier is similar to experimental observation up to phase 3 as defined in Fig. 7.

(iii) The Wang model which is based on Palmgren-Miner's rule predicted the no. of cycles to failure as close to experimental observations

It can therefore be concluded with confidence that the analytical models, such as (i) sectional analysis and (ii) modified Kaar formula can be employed for prediction of load carrying capacity of retrofitted RC beams under static loading and the models Papakonstantinou and Ferrier which were originally developed to address the serviceability of CFRP and GFRP laminates, could also be used for the accurate prediction of the behaviour of cement based composite retrofit system, i.e., UHPFRC as a retrofitting candidate.

Acknowledgments

This paper forms part of UGC-UKERI collaborative project between CSIR-Structural Engineering Research Centre and Cardiff University, UK. Author thank the staff of the Computational Structural Mechanics Group and Structural Testing Laboratory for the co-operation and suggestions provided during the investigation.

References

Alaee, F.J. (2003a), "Fracture model for flexural failure of beams retrofitted with CARDIFRC", *J. Eng. Mech*., **129**, 1028-1038.

Alaee, F.J. and Karihaloo, B.L. (2003), "Retrofitting of reinforced concrete beams with CARDIFRC", *J. Compos. Constr*, **7**, 174-186.

Almusallam, T.H. and Salloum, Y.A. (2001), "Ultimate strength prediction for RC beams externally strengthened by composite materials", *Compos. Part B-Eng*., **32**, 609-619.

Attari, N., Amaziane, S. and Chemrouk, M. (2012), "Flexural strengthening of concrete beams using CFRP, GFRP and hybrid FRP sheets", *Constr. Build. Mater.*, **37**, 746-757.

Bakis C.B., Brown, L., Cosenza, V., Davalos, E. and Lesko, J. (2002), "Fiber-reinforced polymer composites for construction-state of art review", *J. Compos. Constr*., **6**, 73-87.

Balaguru, B. and Shah, S.P. (1982), "A method of predicting crack width and deflections for fatigue loading", *ACI Spec. Publ*., **75**(5), 153-175.

Barenblatt, G.I. (1959), "On equilibrium cracks forming during brittle fracture", *J. Appl. Math. Mech*., **23**, 434-444.

Benson, S.D.P. and Karihaloo, B.L. (2005), "CARDIFRC-Development and mechanical properties. Part I: Development and workability", *Mag. Concrete Res*., **57**(6), 347-352.

Bosco, C. and Carpinteri, A. (1992), "Fracture mechanics evaluation of minimum reinforcement in concrete structures", *Proceedings of the International Workshop on Application of fracture mechanics to reinforced concrete*, Turin, Italy.

Buyukozturk, O. and Hearing, B. (1998), "Failure behavior of pre-cracked concrete beams with FRP", *J. Compos. Constr*., **2-3**, 138-144.

CEB-FIP Model Code (1993), Lausanne, Switzerland.

Cheng, L. (2011), "Flexural fatigue analysis of a CFRP form reinforced concrete bridge deck", *Compos. Struct*., **93**, 2895-2902.

Deng, Z.C. (2005), "The fracture and fatigue performance in flexure of carbon fiber reinforced concrete", *Cement Concrete Compos*., **27,** 131-140.

Dong, J.F., Wang, Q.Y. and Guan, Z.W. (2012), "Structural behavior of RC beams externally strengthened with FRP sheets under fatigue and monotonic loading", *Eng. Struct*., **41**, 24-33.

Dong, Y., Ansari, F. and Karbhari, V.M. (2011), "Fatigue performance of reinforced concrete beams with externally bonded CFRP reinforcement", *Struct. Infrastruct. E*, **7**(3), 229-241.

El-Refai, J. and West, K.S. (2012), "Fatigue of reinforced concrete beams strengthened with externally post-tensioned CFRP tendons", *Constr. Build. Mater*., **29**, 246-256.

Ferrier, E., Bigaud, D., Clement J.C. and Hamelin, P. (2011), "Fatigue-loading effect on RC beams strengthened with externally bonded FRP", *Constr. Build. Mater*., **25**, 539-546.

Guinea, G.V., Pastor, J.Y., Planas, J. and Elices, M. (1998), "Stress intensity factor, compliance and CMOD for a general three-point-bend beam", *J. Fract*., **89**, 103-116.

Hangsoeb, O., Jongsung, S. and Christian, M. (2005), "Fatigue life of damaged bridge deck panels strengthened with carbon fiber sheets", *ACI Struct. J*., **102**(1), 85-92.

Kaar, P.H. and Mattock, A.H. (1963), "High strength bar as concrete reinforcement, Part 4. Control of cracking", *J. PCA Res. Dev. Lab*., **7**(1), 15-38.

Kevin, Z., Arash, E.Z. and Kay, W. (2015), "Rehabilitation of steel bridge girders with corroded ends using ultra-high performance concrete", *Struct. Congr*., 1411-1422.

Lange-Kornbak, D. and Karihaloo, B.L. (1999), "Fracture mechanical prediction of transitional failure and strength of singly-reinforced beams", *Minimum Reinforcement in Concrete Members, ESIS Publication* 24, A. Carpinteri, Ed., Elsevier, London, 31-42.

Leung, C.K.Y., Cheung, Y.N. and Zhang, J. (2007), "Fatigue enhancement of concrete beam with ECC layer", *Cement Concrete Res*., **37**, 743-750.

Leung, C.K.Y. (1998), *Delamination Failure in Concrete Beams Retrofitted with a Bonded Plate*, Fracture Mechanics of Concrete Structures, *AEDIFICATIO Publishers*, Freiburg, Germany, **3**, 1783- 1792.

Liu, F. and Zhou, J. (2016), "Fatigue strain and damage analysis of concrete in reinforced concrete beams under constant amplitude fatigue loading", *Shock Vibr*., **2016**, 73-79.

Manfredi, G. and Pecce, M. (1997), "Low cycle fatigue of RC beams in NSC and HSC", *Eng. Struct*., **19**(3), 217-223.

Nanni, A. (2003), "Concrete repair with externally bonded FRP reinforcement: Examples from Japan", *Concrete Int*., **97**, 22-26.

Papakonstantinou, C.G., Balaguru, P.N. and Petrou, M.F. (2002), "Analysis of reinforced concrete beams strengthened with composites subjected to fatigue loading", *ACI Spec. Publ.*, **206**, 41-60.

Prem, P.R., Ramachandra Murthy, A., Ramesh, G., Bharatkumar, B.H. and Nagesh, R.I. (2015), "Flexural behaviour of damaged RC beams strengthened with ultra-high performance concrete", *Ind. Concrete J*., 2057-2069.

Ramachandra Murthy, A., Karihaloo, B.L., Nagesh, R.I. and Raghu Prasad, B.K. (2013), "Bilinear tension softening diagrams of concrete mixes corresponding to their size-independent specific fracture energy", *Constr. Build Mater*., **47**, 1160-1166.

Shahawy, M. and Beitelman, T.E. (1999), "Static and fatigue performance of RC beams strengthened with CFRP laminates", *J. Struct. Eng*., **125**, 613-625.

Shannag, M.J., Al-Akhras, N.M. and Mahdawi, S.F. (2014), "Flex ure strengthening of lightweight reinforced concrete beams using carbon fibre-reinforced polymers", *Struct. Infrastr. E*, **10**(5), 604-613.

Shin, H.O., Yoon, Y.S. and Cook, W.D. (2015), "Effect of confinement on the axial load response of ultrahigh-strength concrete columns", *J. Struct. Eng*., **141**(6), 04014151-12

Tada, H., Paris, P.C. and Irwin, G.R. (1985), *The Stress Analysis of Cracks-Handbook*, Paris Productions Incorporated, St. Louis, Missouri, U.S.A.

Wang, W., Wu, S.G. and Dai, H.Z. (2006), „Fatigue behaviour and life prediction of carbon fiber reinforced concrete under cyclic flexural loading", *Mater. Sci. Eng. A*, **434**, 347-351.

Wang, W. and Huang, H. (2015), "Fatigue life prediction of RC beams strengthened with externally bonded FRP sheets", *Proceedings of the International Conference on Performance-based and Life-cycle Structural Engineering, Brisbane,* QLD, Australia, 522-528

Xu, S.L., Wang, N. and Zhang, X.F. (2012), "Flexural behavior of plain concrete beams strengthened with ultra-high toughness cementitious composites layer", *Mater. Struct*., **45**, 851-859.

PL